Electronic Supplementary Material (ESI) for Green Chemistry.

Eletronic Supplementary Information (ESI)

Tandem dehydration-transfer hydrogenation reactions of xylose to furfuryl alcohol over zeolite catalysts

Priscilla N. Paulino,[a] Rafael F. Perez,[a,b] Natália G. Figueiredo,[c] and Marco A. Fraga*[a,b]

[a] Instituto Nacional de Tecnologia/MCTIC, Divisão de Catálise e Processos Químicos, Av. Venezuela, 82, sala 518, Saúde, 20081-312, Rio de Janeiro/RJ, Brazil.

[b] Instituto Militar de Engenharia, Praça Gen. Tibúrcio, 80, Urca, 22290-270, Rio de Janeiro/RJ, Brazil

[c] Instituto Nacional de Tecnologia/MCTIC, Divisão de Química Analítica, Av. Venezuela, 82, sala 216, Saúde, 20081-312, Rio de Janeiro/RJ, Brazil.

Correspondig author

Marco A. Fraga.

E-mail: marco.fraga@int.gov.br. Phone: +55-21-2123-1152.

Methodology

N_2 adsorption

Nitrogen adsorption–desorption isotherms were measured at -196 °C on an ASAP 2420. Prior to measurements, the solids were degassed at 350 °C for 12 h under vacuum. The specific surface areas (S_{BET}) were calculated from the N_2 adsorption isotherms using the Brunauer-Emmett-Teller (BET) equation.

XRD

Powder X-ray diffraction (XRD) patterns were collected on a D8 Advance (DaVinci of Bruker) X-ray diffractometer equipped with an Lynxeye detector and a Cu Ka X-ray source (1,5406 Å). The diffraction patterns were measured from 10° to 50° at a scan rate of 0.02°.s^{-1} with a step size of 0.5°.

XRF

Si/Al ratio of the zeolites was determined by X-ray fluorescence spectrometry. The catalysts were analyzed on a Bruker model S8 Tiger by the scanning method.

Titration

The total acidity was determined following the procedure employed by DAVIS *et al*., 2014.[1] 0.01 mol.L^{-1} NaOH solution with 0.1 mol.L^{-1} KCl was prepared and standardized with 0.01 mol.L^{-1} potassium biphthalate. Thereafter, a 0.01 mol.L^{-1} HCl solution was prepared and standardized with the solution prepared above. 10 mg of the catalyst was weighed and sonicated in 15mL of NaOH/KCl solution. This sample was titrated under magnetic stirring with HCl until neutralization (pH 7). The pH was measured with digital pH meter. This procedure was performed in triplicate.

HRMS

Detection of the furanic compounds was performed using the LTQ Orbitrap XL (Thermo Fisher) mass spectrometer with an electrospray-ionization source in positive ionization mode. Scan range for each acquisition was m/*z* 50–1000. The method included full scan event with resolution 30,000 programmed for 10 ms maximum injection time. Instrument parameters were: sheath gas flow rate (40 arbitrary units), discharge current (5.4 µA), capillary temperature (275°C), capillary voltage (42 V), tube lens voltage (110 V). These parameters were determined by analyzing each analytical standard and the fractions separated from the

reaction aliquots. They were all prepared in acidified water (formic acid 0.1%) before infusion. Data analysis included Xcalibur 3.0 program (Thermo Fisher) and fragment prediction using the MassFrontier 7.0 (Thermo Fisher) program. Identification was considered when mass errors values were less than 5 ppm and at least 2 exact match fragments were found in the fragment ion search (FISh) annotation based on the proposed structures.

Catalytic tests

The aliquots were analyzed by high performance liquid chromatography (HPLC) in a Waters equipment, model Alliance e2695, coupled to a photodiode array (model 2998) and a refractive index (model 2414) detectors. The HPLC apparatus was equipped with an Aminex HPX-87H column (Bio-Rad Laboratories) and used at 65 °C with 5 mmol.L^{-1} H_2SO_4 as an eluent at a flow rate of 0.7 mL min^{-1}.Commercial standards were used to identify each product. After analysis of the aliquots, it was possible to calculate conversion, selectivity and yield to the products. The formulas used for calculation were presented in Equations 1-3.

$$Xylose\ conversion\ (X) = \frac{[xylose]_i - [xylose]_f}{[xylose]_i} x100 \quad (1)$$

$$Selectivity\ (S) = \frac{[product]}{[xylose]_i - [xylose]_f} x100 \quad (2)$$

$$Yield\ (Y) = \frac{[product]}{[xylose]_i} x100 \quad (3)$$

Characterization

N_2 adsorption–desorption isotherms of the zeolites are shown in Figure S1. All catalysts revealed their microporous properties with type I isotherms and type IV hysteresis.[2]

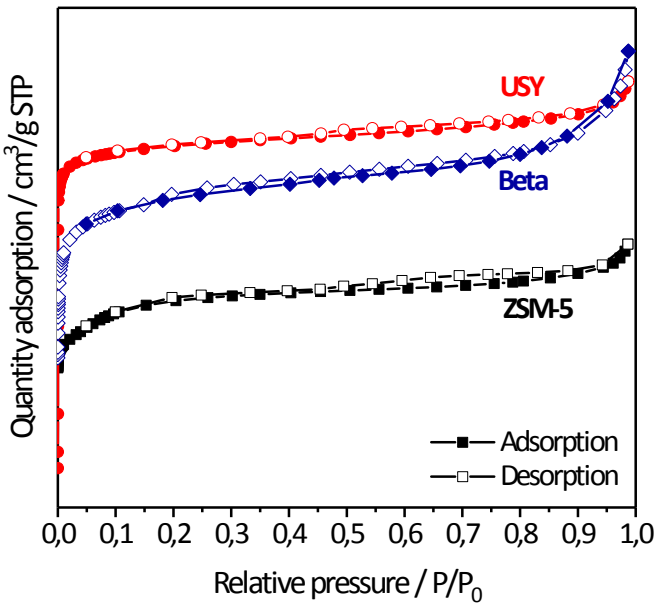

Figure S1. Nitrogen adsorption/desorption isotherms of zeolites samples.

Zeolite X-ray diffractograms are shown in Figure S2. It is possible to verify a typical diffractogram of an MFI structure for ZSM-5 sample, with main diffraction peaks at 2θ = 10.16°, 11.33°, 23.08°, 23.48° and 23.78° (PDF 37-0359).[3]

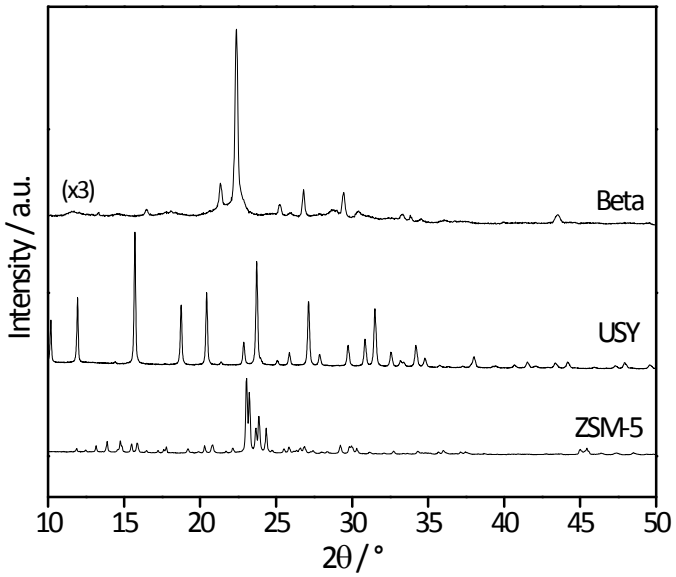

Figure S2. XRD patterns of ZSM-5, USY and Beta zeolites.

Beta zeolite presented more intense diffraction peaks at 2θ = 7.6° and 22.4° (PDF 47-0183). The synthesis procedure successfully led to zeolite Beta, corresponding to a structure of the BEA family.[4] Zeolite USY presented a characteristic diffractogram of FAU family structure with main diffraction peaks at 2θ = 15.28°, 20.21°, 24.32°, (PDF 39-1380).[5]

The ESI (+) HRMS spectra allowed the unequivocal identification of the furanic compounds with less than 5 ppm error (Table 1). Applying the Thermo Scientific™ HighChem MassFrontier 7.0 Spectral Interpretation Software tool, fragments structures were proposed and searched in the mass spectrum to match the compounds identification (Figure S3, Figure S4 and Figure S5).

Table 1. ESI(+)–HRMS data.

	Protonated form	**Theoretical *m/z***	**Experimental *m/z***	**Error (ppm)**
Furfural	$[C_5H_5O_2]^+$	97.02841	97.02888	4.8
Furfuryl Alcohol	$[C_5H_7O_2]^+$	99.04406	99.04449	4.3
Glycerol	$[C_3H_9O_3]^+$	93.05462	93.05499	3.9

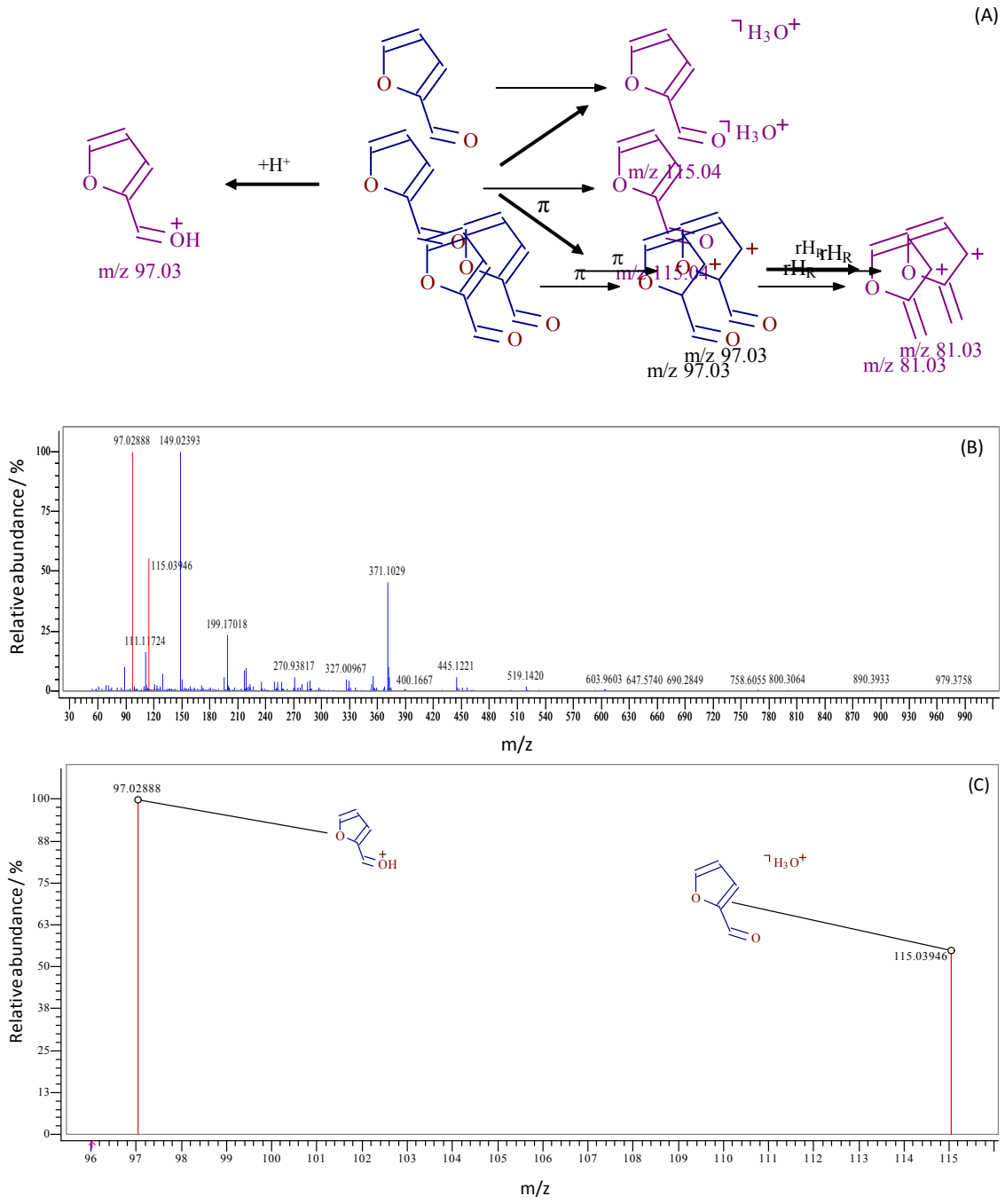

Figure S3. (A) Proposed structures for furfural fragmentation as given by Thermo Scientific™ HighChem Mass Frontier 7.0 Spectral Interpretation Software; (B) ESI (+) High-resolution mass spectrometry (HRMS) of furfural (m/z 97,02888) highlighting the structure matched ions (m/z 115,03946 and m/z 97,02888); (C) Experimental fragments that were accounted by the Mass Frontier predictive algorithm.

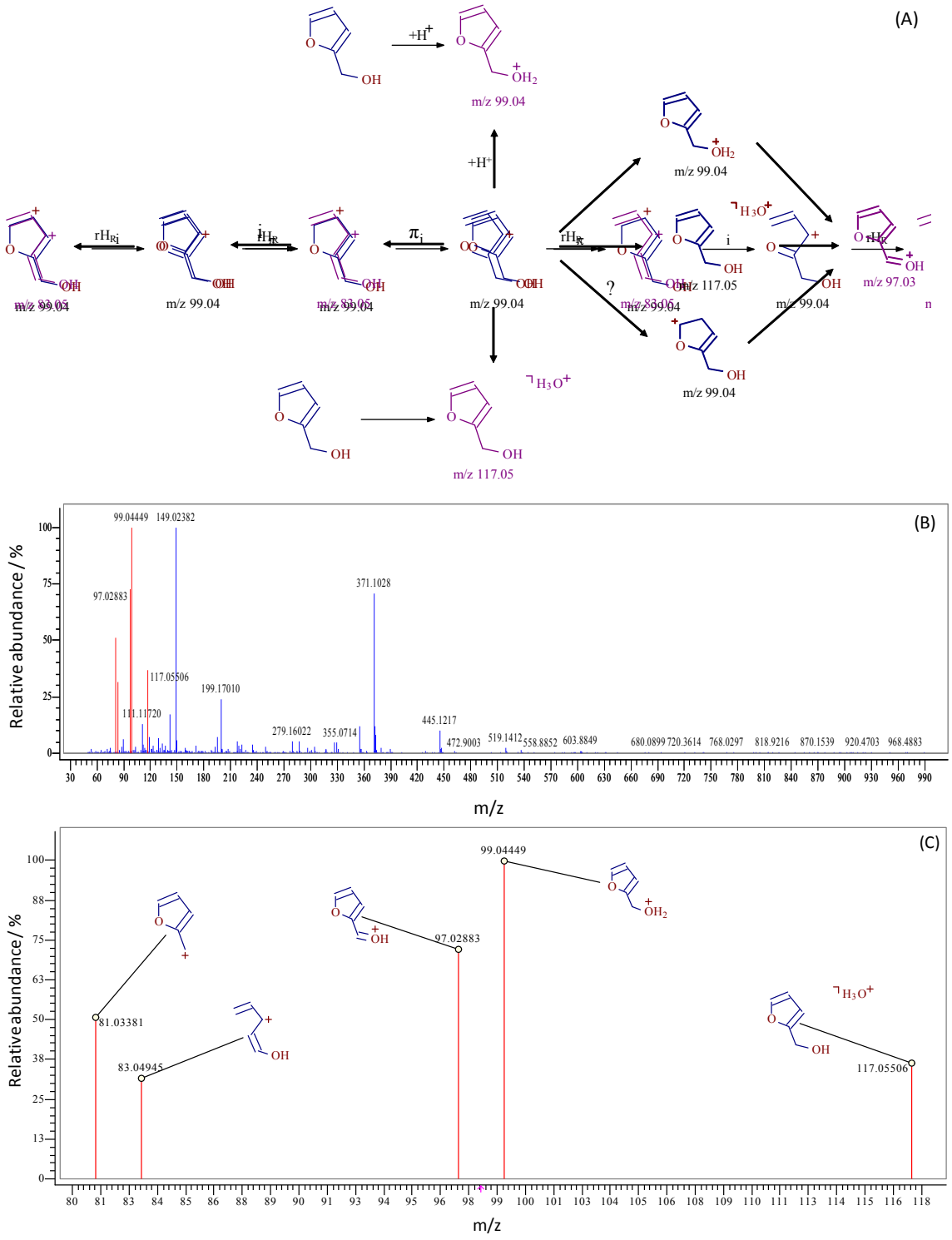

Figure S4. (A) Proposed structures for furfuryl alcohol fragmentation as given by Thermo Scientific™ HighChem Mass Frontier 7.0 Spectral Interpretation Software; (B) ESI (+) High-resolution mass spectrometry (HRMS) of furfuryl alcohol (m/z 99,04449) highlighting the structure matched ions (m/z 117,05506; m/z 99,04449; m/z 97,02883; m/z 83,04945 and m/z 81,03381); (C) Experimental fragments that were accounted by the Mass Frontier predictive algorithm.

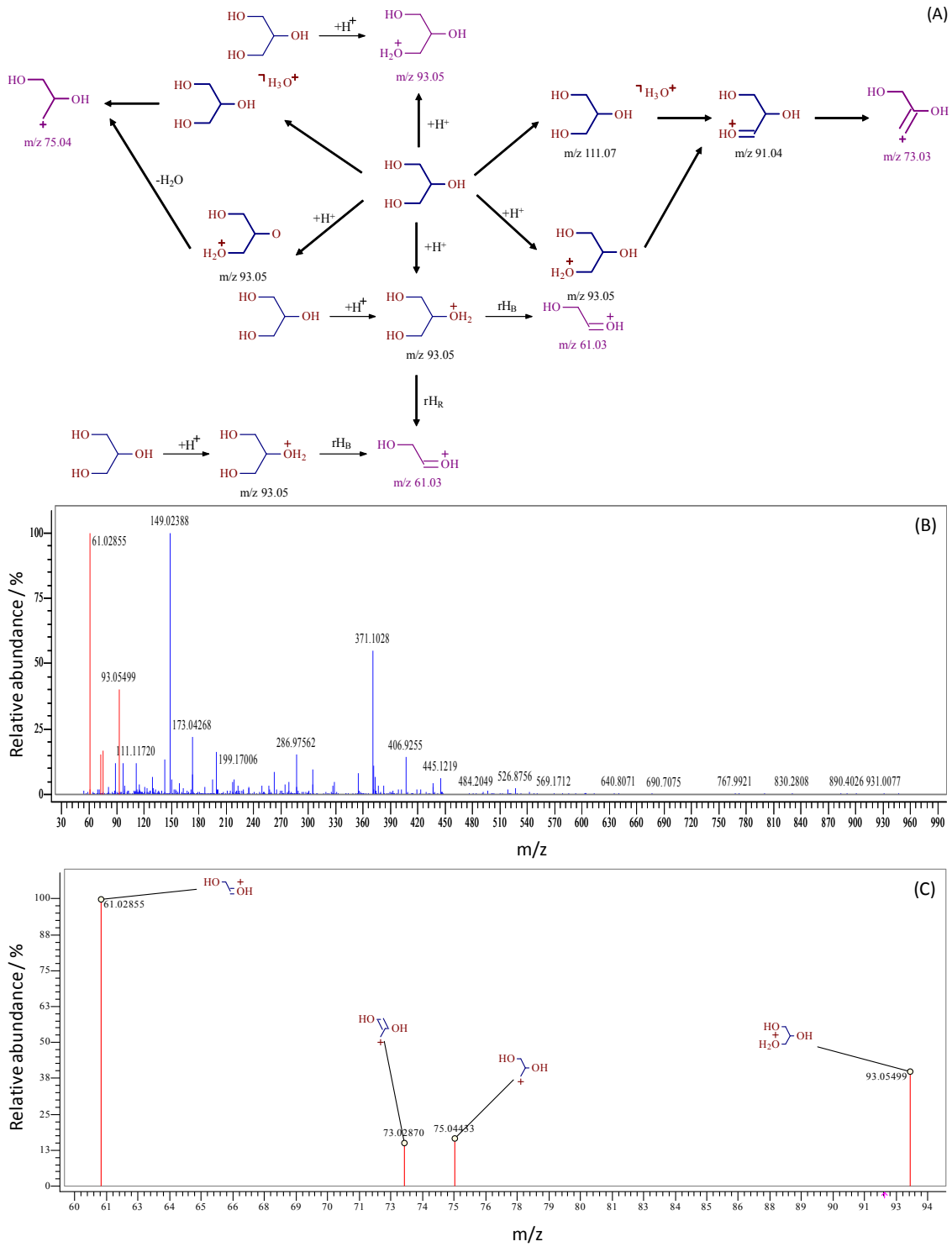

Figure S5. (A) Proposed structures for glycerol fragmentation as given by Thermo Scientific™ HighChem Mass Frontier 7.0 Spectral Interpretation Software; (B) ESI (+) High-resolution mass spectrometry (HRMS) of glycerol (m/z 93,05499) highlighting the structure matched ions (m/z 93,05499; m/z 75,04433; m/z 73,02870; m/z 61,02855); (C) Experimental fragments that were accounted by the Mass Frontier predictive algorithm.

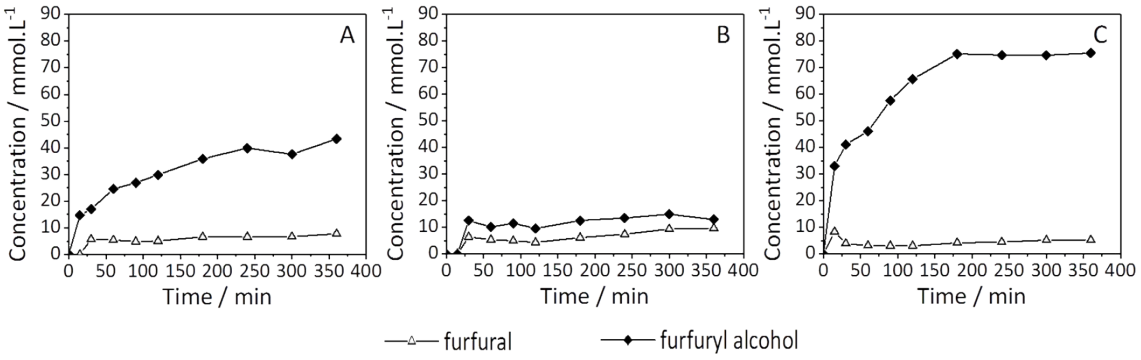

Figure S6. Concentration evolution of furfural and furfuryl alcohol on (A) ZSM-5, (B) USY and (C) zeolite Beta.

After the reaction, the preservation of zeolite Beta crystalline structure was assessed by XRD. The patterns of fresh and post-reaction zeolite Beta are presented in Figure S7. Note that after the reaction with H_2O:IPA = 1:1 the structure remained intact, indicating its stability to the hemicellulosic biomass conversion reaction.

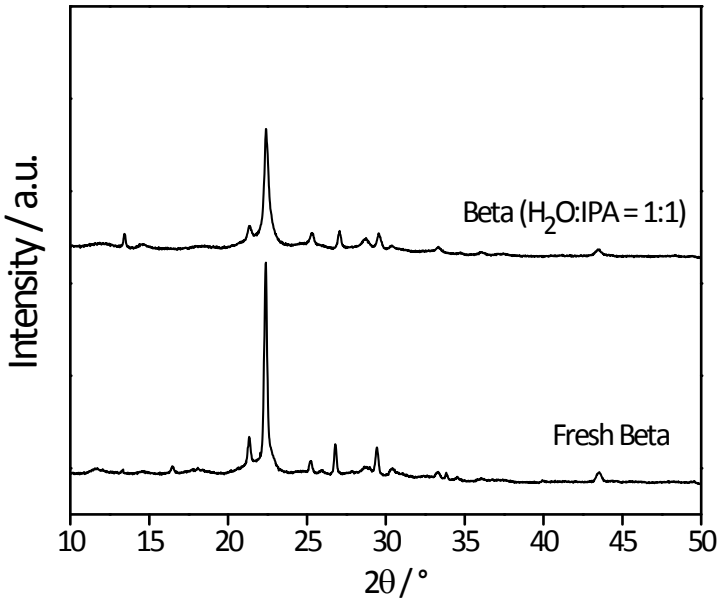

Figure S7. XRD of fresh and after reaction (H_2O:IPA = 1:1) Beta zeolite.

Supplementary references

1. S. E. Davis, A. D. Benavidez, R. W. Gosselink, J. H. Bitter, K. P. de Jong, A. K. Datye and R. J. Davis, *J Mol Catal A Chem*, 2014, **123**, 388.

2. M. Thommes, K. Kaneko, A. V. Neimark, J. P. Olivier, F. Rodriguez-Reinoso, J. Rouquerol and K. S. W. Sing, *Pure Appl. Chem.*, 2015, **87**, 1051.

3. M. Moreno-Recio, J. Santamaría-González and P. Maireles-Torres, *Chem. Eng. J.*, 2016, **303**, 22.

4. J. Zhang, P. Cao, H. Yan, Z. Wu and T. Dou, *Chem. Eng. J.*, 2016, **291**, 82.

5. A. Sachse, C. Wuttke, U. Díaz and M. O. de Souza, *Micropor. Mesopor. Mat.*, 2015, **217**, 81.